ORIGINAL RESEARCH

Identification of Hic–5 as a Novel Scaffold for the MKK4/p54 JNK Pathway in the Development of Abdominal Aortic Aneurysms

Xiao-Feng Lei, PhD; Joo-ri Kim-Kaneyama, PhD; Shigeko Arita-Okubo, BSc; Stefan Offermanns, MD, PhD; Hiroyuki Itabe, PhD; Takuro Miyazaki, PhD; Akira Miyazaki, MD, PhD

Background—Although increased amounts of reactive oxygen species in the pathogenesis of abdominal aortic aneurysm (AAA) are well documented, the precise molecular mechanisms by which reactive oxygen species induce AAAs have not been fully elucidated. This study focused on the role of hydrogen peroxide–inducible clone 5 (Hic-5), which is induced by hydrogen peroxide and transforming growth factor-β, in the cellular signaling of AAA pathogenesis.

Methods and Results—Using the angiotensin II–induced AAA model in *Apoe*$^{-/-}$ mice, we showed that *Apoe*$^{-/-}$*Hic-5*$^{-/-}$ mice were completely protected from AAA formation and aortic rupture, whereas *Apoe*$^{-/-}$ mice were not. These features were similarly observed in smooth muscle cell–specific Hic-5–deficient mice. Furthermore, angiotensin II treatment induced Hic-5 expression in a reactive oxygen species–dependent manner in aortic smooth muscle cells in the early stage of AAA development. Mechanistic studies revealed that Hic-5 interacted specifically with c-Jun N-terminal kinase p54 and its upstream regulatory molecule mitogen-activated protein kinase kinase 4 as a novel scaffold protein, resulting in the expression of membrane type 1 matrix metalloproteinase and matrix metalloproteinase 2 activation in aortic smooth muscle cells.

Conclusion—Hic-5 serves as a novel scaffold protein that specifically activates the mitogen-activated protein kinase kinase 4/p54 c-Jun N-terminal kinase pathway, thereby leading to the induction and activation of matrix metalloproteinases in smooth muscle cells and subsequent AAA formation. Our study provided a novel therapeutic option aimed at inhibiting the mitogen-activated protein kinase kinase 4–Hic-5–p54 c-Jun N-terminal kinase pathway in the vessel wall, particularly through Hic-5 inhibition, which may be used to produce more precise and effective therapies. **(*J Am Heart Assoc*. 2014;3:e000747 doi: 10.1161/JAHA.113.000747)**

Key Words: aneurysm • Hic-5 • JNK-signaling scaffold protein • smooth muscle

Abdominal aortic aneurysm (AAA) is an age-associated disease that affects approximately 5% of elderly individuals and is responsible for a significant number of deaths in Western countries.[1] Oxidative stress, generated by excessive reactive oxygen species (ROS), has been shown to play causal roles in AAAs.[2,3] Animal models deficient in ROS-generating enzymes, such as inducible nitric oxide synthase, NADPH oxidase-1, and p47phox, clearly demonstrated preserved aortic wall morphology and attenuated AAA development.[4–6] Increased activities of matrix metalloproteinases (MMPs) play a key mechanical role in the formation of AAAs.[7,8] A strong mechanistic link exists between increased ROS production and MMP activity. As has been reported recently, angiotensin II (Ang II) induces the generation of ROS in vascular smooth muscle cells (VSMCs), which triggers the activation of MMPs and vascular inflammatory responses, thereby promoting the formation of AAAs in an animal model.[2,9] However, little is known about the detailed signaling pathways that regulate these processes.

Hydrogen peroxide–inducible clone 5 (Hic-5), originally identified as a gene induced by H_2O_2 as well as transforming growth factor-β1 (TGF-β1), has been shown to serve as a focal adhesion protein that belongs to the paxillin family.[10] We recently successfully generated Hic-5–deficient mice, which were viable and fertile and had no obvious abnormalities.[11]

From the Department of Biochemistry, Showa University School of Medicine, Tokyo, Japan (X.-F.L., J.K.-K., S.A., T.M., A.M.); Division of Biological Chemistry, Departments of Molecular Biology, Showa University School of Pharmacy, Tokyo, Japan (H.I.); Department of Pharmacology, Max-Planck-Institute for Heart and Lung Research, Bad Nauheim, Germany (S.O.).

Correspondence to: Joo-ri Kim-Kaneyama, PhD, Department of Biochemistry, Showa University School of Medicine, 1-5-8 Hatanodai, Shinagawa-ku, Tokyo 142-8555, Japan. E-mail: shuri@pharm.showa-u.ac.jp

Received January 5, 2014; accepted March 5, 2014.

The molecular basis of Hic-5 and its implications in various pathophysiological conditions including vascular remodeling have already been described.[11,12] However, whether Hic-5 is involved in AAA formation is unknown. In this study, we analyzed the potential role of Hic-5 in AAA formation. We found that AAA formation and rupture were almost completely prevented in Hic-5–deficient mice. Mechanistic studies showed that Hic-5 served as a novel scaffold protein to regulate c-Jun N-terminal kinase (JNK) pathway activation, which resulted in MMP expression and activation in VSMCs and the subsequent formation of AAAs.

Methods

Generation of Mice

All experiments were conducted in accordance with the protocols approved by the Institutional Committee for Animal Research of Showa University. All of the mice were bred in C56BL/6 background genotype. *Apoe*$^{-/-}$*Hic-5*$^{-/-}$ mice were generated by crossing *Hic-5*$^{-/-}$ mice with *Apoe*$^{-/-}$ mice. For the generation of smooth muscle (SM)–specific knockout mice for Hic-5 (SM-Hic-5KO), we used our previously produced mouse strain in which all exons of Hic-5 were floxed (*Hic-5*$^{F/F}$).[11] *Hic-5*$^{F/F}$ mice were intercrossed with a transgenic mouse line expressing inducible SM-specific Cre recombinase with a modified estrogen receptor binding domain (CreER^{T2}) under the control of the SM-specific SM myosin heavy chain promoter (SMMHC).[13] The SMMHC-Cre gene is located on the Y chromosome in this mouse line, and only male offspring carried the SMMHC-Cre gene. The *Hic-5*$^{F/F}$*/SMMHC-Cre*$^{Y+}$ (*Hic-5*$^{F/F}$*/sCre*$^{Y+}$) mice strain was used. *Apoe*$^{-/-}$ *Hic-5*$^{F/F}$*/sCre*$^{Y+}$ mice were generated by crossing *Hic-5*$^{F/F}$*/sCre*$^{Y+}$ mice with *Apoe*$^{-/-}$ mice. Male *Hic-5*$^{F/F}$*/sCre*$^{Y+}$ mice (5 to 6 weeks old) were injected with tamoxifen (1 mg/day IP) on 5 consecutive days. The day of the last tamoxifen injection was defined as day 0. The Ang II treatment was performed for 4 weeks from day 55 after the tamoxifen injection. All animals were housed under a 12-hour light/12-hour dark regimen and consumed on a normal chow diet.

The Mouse Model of Ang II–Induced Aortic Aneurysm

The mouse model of Ang II–induced aneurysm formation has been previously described.[14] Ang II was infused via the use of ALZET model 2004 osmotic pumps (ALZA Corp) at 1000 ng/kg per minute. After 4 weeks of infusion, aneurysm size was evaluated by measuring maximal abdominal aortic diameters with a digital caliper. Systolic blood pressure was measured in conscious mice by using the tail-cuff method (MK-2000; Muromachi Kikai Co). Serum total cholesterol concentrations were determined by using a cholesterol determination kit (Wako Chemicals).

Histological Analysis

After the animals were killed, their aortas were perfused with 10% phosphate-buffered formalin for 5 minutes. Whole aortas were harvested and fixed with 10% formalin for 24 hours. The aortas were cut and embedded in paraffin or OCT compound for the preparation of cross sections (5 μm). Paraffin sections were stained with hematoxylin and eosin (H&E) staining and Victoria Blue H&E staining or used for immunostaining. Frozen sections were used for immunofluorescence.

Immunohistochemistry

Formaldehyde-fixed paraffin sections and frozen sections were incubated with primary antibodies overnight at 4°C. The primary antibodies used were Hic-5 monoclonal (BD Biosciences), α-SM actin monoclonal (Sigma-Aldrich), and rat anti-mouse macrophage-monocyte specific monoclonal (AbD Serotec). As a negative control, isotype-matched antibodies were used in place of the primary antibodies. Slides were viewed with use of a microscope (IX70; Olympus) and digital camera (DP72; Olympus). Immunofluorescence images were captured and analyzed with Lumina vision software (Mitani Visual System).

Harvest of Mouse Aortic VSMCs

The preparation of mouse aortic VSMCs was performed as previously described.[11] In brief, aortas were isolated from *Hic-5*$^{+/+}$ and *Hic-5*$^{-/-}$ mice, followed by separation of tunica media from the adventitia and endothelium. The cells were dispersed in collagenase and elastase and maintained in Dulbecco's modified Eagle's medium. Passage 2 to 8 VSMCs were used for experiments.

Western Blotting

VSMCs were harvested on ice-cold lysis buffer. In some experiments, VSMCs were infected with adenovirus encoding *Hic-5* (Ad-hic-5/flag) or β-galactosidase (Ad-β-gal) as a control. Aortic tissue samples were crushed with a biomasher (Nippi) and lysed in lysis buffer. Equal amounts of protein were separated by 10% SDS-PAGE. Immunodetection was performed using the following primary antibodies: Hic-5; GAPDH and MMP2 (Santa Cruz Biotechnology), membrane type 1 (MT1)-MMP (Sigma-Aldrich); extracellular signal-regulated kinase (ERK), p38, mitogen-activated protein kinase kinase (MAPKK; also known as MKK) 4, MKK7, and their

phosphorylated (P) forms (P-ERK, P-p38, P-MKK4, P-MKK7, and P-JNK1/2) (Cell Signaling); and JNK1/2 (Santa Cruz Biotechnology). The densities of the bands were measured using Light-Capture and Densitograph software (AE-6962FC, CS Analyzer version 2.0; ATTO).

Gelatin Zymography and In Situ Zymography

The evaluation of MMP activities in response to Ang II was performed as described previously.[9,15] To analyze the role of Hic-5 in Ang II–induced MMP activation, VSMCs were treated with Ang II (1 μmol/L) for 24 hours. Aortas from *Apoe*$^{-/-}$ and *Apoe*$^{-/-}$*Hic-5*$^{-/-}$ mice infused with Ang II for 7 days were incubated in culture medium for 20 hours. The medium was then collected and centrifuged to remove cell debris. The conditioned medium was concentrated and electrophoresed in SDS-PAGE gels containing gelatin (Sigma-Aldrich). Gels were washed in 2.5% Triton X-100 and incubated overnight in zymography buffer (50 mmol/L Tris, pH 7.4, 10 mmol/L $CaCl_2$) at 37°C. Gels were subsequently stained with Coomassie brilliant blue. For in situ zymography, freshly cut frozen aortic sections (10 μm) were incubated with a fluorogenic gelatin substrate (DQ gelatin; Invitrogen) dissolved to 25 mg/mL in zymographic buffer. Proteolytic activity was detected as green fluorescence with microscopy (IX70; Olympus, Japan). Negative control zymograms were incubated in the presence of 5 mmol/L EDTA.

Immunoprecipitation

Aortic media were lysed in RIPA buffer containing a mixture of proteinase inhibitors and 1 mmol/L sodium vanadate for immunoprecipitation studies. Dynabeads (Invitrogen) conjugated with an antibody against Hic-5 or control mouse IgG (Santa Cruz Biotechnology) were added to the lysates (5 μg per sample) and rotated at room temperature for 60 minutes. Samples were washed with RIPA buffer 3 times and soaked in elution buffer for 10 minutes. Immunoprecipitated proteins were then processed for SDS-PAGE and Western blot analysis.

In Situ Proximity Ligation Assay

The in situ proximity ligation assay (PLA) method allows the subcellular colocalization of protein–protein interactions to be determined.[16,17] Mouse VSMCs were cultured in cover glasses. After culture in serum-free medium for 24 hours, VSMCs were treated with or without Ang II for 10 minutes. VSMCs were then washed in PBS and fixed with 4% paraformaldehyde for 15 minutes. PLA assays were performed as recommended by the manufacturer (OLink Biosciences). Red fluorescent spots were then visualized with microscopy (IX70; Olympus). The negative control was performed without primary antibodies.

Electron Microscopic Observations

Immunoelectron microscopy was performed as previously described.[11] Briefly, sections of mouse aortas were incubated overnight with primary antibodies at 4°C. After the sections were washed with PBS, 10-nm gold-labeled sheep anti-mouse IgG and 15-nm gold-labeled goat anti-rabbit IgG secondary antibodies (BBI International) were used; subsequently, sections were evaluated with Hitachi H-7600 transmission electron microscope.

Statistical Analyses

The data are presented as mean±SEM. Statistical tests including the Mann–Whitney test (for comparisons of parameters among 2 groups), Gehan-Breslow-Wilcoxon test (for survival curves), Fisher's exact test (for aneurysm incidence), and 2-way ANOVA using the Bonferroni posttests (for comparisons of different parameters between 2 genotypes) were performed using GraphPad Prism (version 5.0 for Mac) software. $P<0.05$ was considered statistically significant.

Results

Hic-5 Deficiency Suppressed Ang II–Induced AAA Formation and AAA Rupture

Ang II infusion for 4 weeks induced AAA formation in *Apoe*$^{-/-}$ mice.[14] Here, we used *Apoe*$^{-/-}$ mice and *Apoe*$^{-/-}$*Hic-5*$^{-/-}$ mice to investigate the role of Hic-5 in the pathogenesis of Ang II–induced AAAs. Ang II infusion increased systolic blood pressure in both groups to the same extent (Table). No significant difference in cholesterol levels was observed between these 2 groups after Ang II infusion (Table).

No aneurysm was detected in either group after saline infusion (Figure 1A). Ang II infusion markedly induced AAAs in 87% (13/15) of *Apoe*$^{-/-}$ mice (Figure 1A and 1C), while only 11% (1/9) of *Apoe*$^{-/-}$*Hic-5*$^{-/-}$ mice developed small AAAs. We also noted that maximal aortic diameter (Figure 1B and 1D) was significantly smaller in *Apoe*$^{-/-}$*Hic-5*$^{-/-}$ mice than in *Apoe*$^{-/-}$ mice. Interestingly, over the 4 weeks of the experiment, 40% (6/15) of the *Apoe*$^{-/-}$ mice infused with Ang II died in the first week, whereas none of the *Apoe*$^{-/-}$*Hic-5*$^{-/-}$ mice died during the entire experiment (Figure 1E). *Apoe*$^{-/-}$ mice showed arterial rupture and massive bleeding in the abdominal cavities (Figure 1F and 1G). In Victoria Blue H&E staining, which specifically demonstrates elastic fibers in the background of H&E-stained tissues, the elastic lamina was

Table. Systolic Blood Pressure and Total Cholesterol Levels of *Apoe*$^{-/-}$, *Apoe*$^{-/-}$*Hic-5*$^{-/-}$ and *Apoe*$^{-/-}$*Hic-5*$^{F/F}$*/sCre*$^{Y+}$ Mice

Mice	Systolic Blood Pressure, mm Hg		Total Cholesterol, mg/dL (Ang II Infusion)
	Before Treatment	Ang II Infusion	
Apoe$^{-/-}$	109.5±5.7	140.2±9.7*	651.2±81.8
Apoe$^{-/-}$*Hic-5*$^{-/-}$	104.4±7.9	136.8±12.3*,†	615.4±104.4†
Apoe$^{-/-}$ (tamoxifen)	108±8.5	141.4±9.6*	524.1±106.7
Apoe$^{-/-}$*Hic-5*$^{F/F}$*/sCre*$^{Y+}$ (tamoxifen)	109±10.7	135.9±10.6*,†	518.7±73.7†

*P<0.01 versus before Ang II treatment.
†No significant difference between *Apoe*$^{-/-}$ and *Apoe*$^{-/-}$*Hic-5*$^{-/-}$ or *Apoe*$^{-/-}$*Hic-5*$^{F/F}$*/sCre*$^{Y+}$ mice.

extensively disrupted and degraded in *Apoe*$^{-/-}$ mice. In contrast, Hic-5 deficiency completely prevented the elastic lamina from degradation (Figure 1G). These results suggest that protection from elastin degradation is a key mechanism for the inhibition of Ang II–induced AAA formation in *Apoe*$^{-/-}$*Hic-5*$^{-/-}$ mice.

VSMC-Derived Hic-5 Was Required for AAA Formation

We first investigated the expression of Hic-5 in aortic tissues from normal and Ang II–infused *Apoe*$^{-/-}$ mice. Consistent with our previous report,[12,18] Hic-5 was highly expressed in SM cells (SMCs) in addition to endothelium (Figure 2A) but not in macrophages in the aortas of *Apoe*$^{-/-}$ mice after the Ang II treatment for 7 days or 4 weeks (Figure 2B and 2C). The expression pattern of Hic-5 was similar to that of α-SM actin in both normal aorta and AAA lesions, which was consistent with our previous report.[18] Although macrophages have been reported to have a crucial role in the development of Ang II–induced AAAs,[19] Hic-5 was not detected by immunostaining in the macrophages of AAA lesions (Figure 2B) or by Western blotting analyses in cultured macrophages (data not shown).

To obtain direct evidence for the key role of VSMC-derived Hic-5 in AAA formation, we created SM-specific *Hic-5* knockout mice (SM-Hic-5 KO). We used a transgenic mouse line, which expressed in an SMC-specific manner a tamoxifen-inducible Cre recombinase under the control of the SMMHC promoter,[13] bred to the well-established *Hic-5*^{floxed} mouse line.[11] *Hic-5*$^{flox/flox}$*/SMMHC-Cre*$^{Y+}$ (*Hic-5*$^{F/F}$*/sCre*$^{Y+}$) mice (see "Methods" for details) were treated with tamoxifen as shown in Figure 3A. As a control, we used *Hic-5*$^{F/F}$*/sCre*$^{Y+}$ mice to which tamoxifen was not administered. The successful SMC-specific deletion of Hic-5 in the aortic media was shown by Western blotting after the tamoxifen treatment (Figure 3B). Cre expression in this mouse line has previously been shown to be specific for vascular and visceral SMCs.[13] We also noted that tamoxifen treatment suppressed Hic-5 expression in the colon (Figure 3B) but not in the lung. Hic-5 was expressed mainly in the endothelium and pneumocytes rather than SMCs in the mouse lung (data not shown).

By crossing male *Hic-5*$^{F/F}$*/sCre*$^{Y+}$ mice with female *Apoe*$^{-/-}$ mice, *Apoe*$^{-/-}$*Hic-5*$^{F/F}$*/sCre*$^{Y+}$ mice were generated. The Ang II treatment was performed from day 55 after the tamoxifen injection (Figure 3A) using tamoxifen-injected *Apoe*$^{-/-}$ mice as a control. The successful SMC-specific deletion of Hic-5 in tamoxifen-injected *Apoe*$^{-/-}$*Hic-5*$^{F/F}$*/sCre*$^{Y+}$ mice was confirmed with use of Western blotting assay of the aortic media after the Ang II treatment, which showed a 98% reduction in Hic-5 protein levels after the tamoxifen treatment (Figure 3D). In contrast, Hic-5 expression in the aortic media from *Apoe*$^{-/-}$ mice was not affected by tamoxifen. Systolic blood pressure and total cholesterol levels were not significantly different between the 2 groups (Table). Although total cholesterol levels were decreased after the tamoxifen treatment in *Apoe*$^{-/-}$ mice, as previously reported,[20] treatment of *Apoe*$^{-/-}$ mice and tamoxifen-injected *Apoe*$^{-/-}$ mice with Ang II for 4 weeks induced AAA formation (13/15 and 5/7, respectively) and AAA rupture (6/15 and 3/7, respectively) to the same extent. However, in contrast to tamoxifen-injected *Apoe*$^{-/-}$, a marked reduction in AAA rupture (0/8), AAA formation (1/8), and maximal aortic diameter was observed in tamoxifen-injected *Apoe*$^{-/-}$*Hic-5*$^{F/F}$*/sCre*$^{Y+}$ mice (Figure 3C, 3E through 3G). These results suggest that the loss of Hic-5 expression in aortic VSMCs, but not other aortic wall cells, is crucial for Ang II–induced AAA formation.

We next examined the effects of Ang II on Hic-5 expression in the aorta from *Apoe*$^{-/-}$ mice and cultured aortic VSMCs. Hic-5 levels in aortic tissues were significantly enhanced in *Apoe*$^{-/-}$ mice in the early stage of Ang II infusion (Figure 4A). Hic-5 expression was also increased by Ang II in a concentration-dependent manner in cultured mouse aortic VSMCs (Figure 4B). As was previously reported, Ang II increased the amount of NADPH oxidase–derived ROS in aortic VSMCs.[21,22] Pretreatment with ROS scavenger *N*-acetyl-L-cysteine markedly reduced Ang II–induced Hic-5 expression (Figure 4B).

Hic-5 Deficiency Prevented Ang II–Induced MMP Expression and Activation in VSMCs

Among the MMPs, VSMC-derived MMP-2, which is cleaved by MT1-MMP into active MMP2, and macrophage-derived MMP9 were shown to work in concert to degrade extracellular matrix, thereby promoting AAA formation and rupture.[7,23] Ang II has been shown to stimulate the secretion and activation of MMP2 in VSMCs during AAA formation.[9,24,25] Ang II infusion

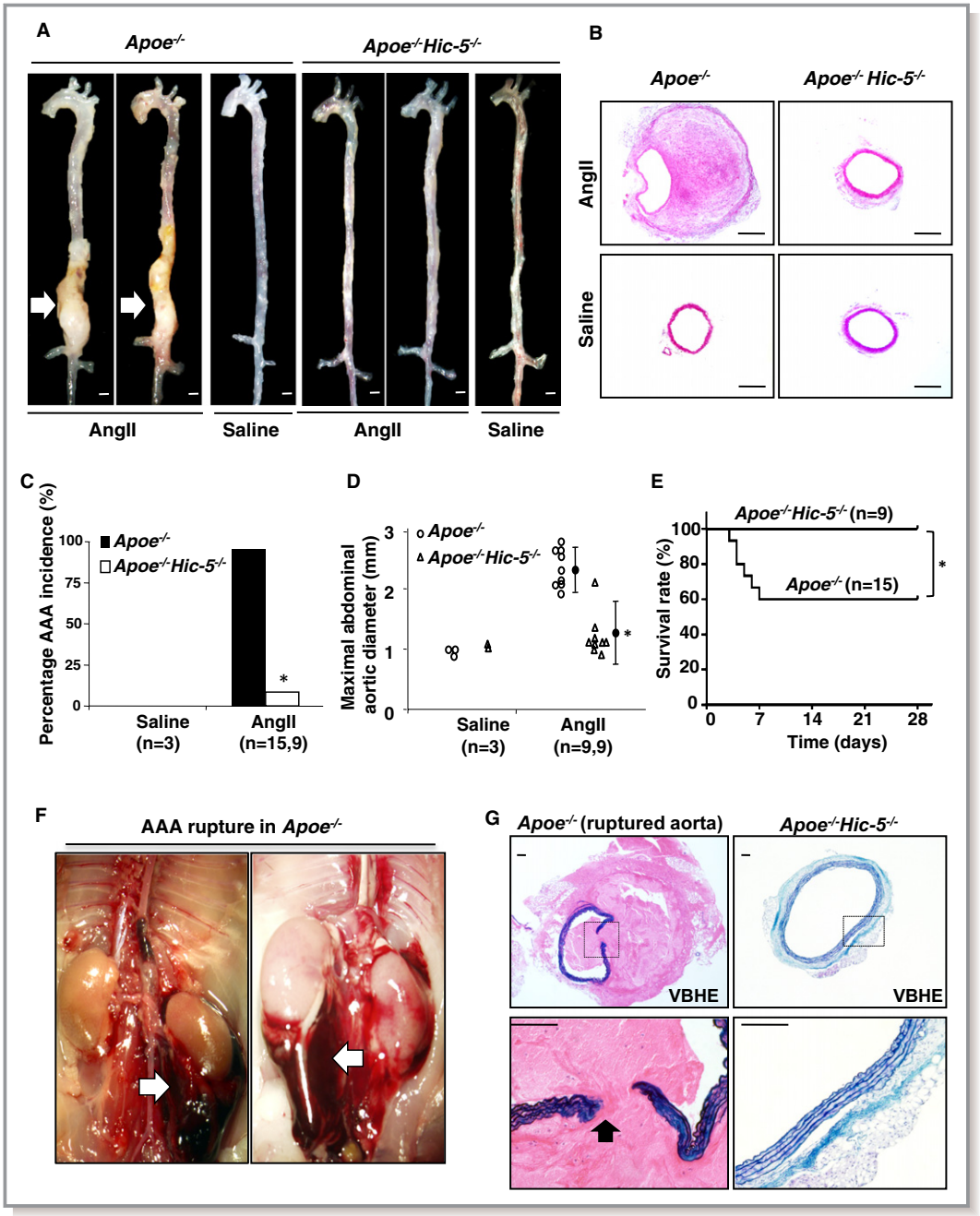

Figure 1. Hic-5 deficiency blocked Ang II–induced AAA formation and AAA rupture in vivo. *Apoe*$^{-/-}$ and *Apoe*$^{-/-}$*Hic-5*$^{-/-}$ mice were treated with Ang II or saline for 4 weeks. A, Representative aortas from mice treated with saline or Ang II. The arrows point to typical AAAs in *Apoe*$^{-/-}$ mice. Scale bars, 1 mm. B, Hematoxylin and eosin (H&E [HE]) stains of aortic cross sections from *Apoe*$^{-/-}$ and *Apoe*$^{-/-}$*Hic-5*$^{-/-}$ mice after saline or Ang II infusion for 4 weeks. Scale bars, 500 μm. C, The incidence of Ang II–induced AAAs in *Apoe*$^{-/-}$ (n=15) and *Apoe*$^{-/-}$*Hic-5*$^{-/-}$ mice (n=9). No AAA formation was observed in the control groups (saline treatment) in both *Apoe*$^{-/-}$ (n=3) and *Apoe*$^{-/-}$*Hic-5*$^{-/-}$ mice (n=3). *P<0.05, significantly different from Ang II–infused *Apoe*$^{-/-}$ mice. D, Maximal diameters of the abdominal aortas of *Apoe*$^{-/-}$ and *Apoe*$^{-/-}$*Hic-5*$^{-/-}$ mice after the Ang II treatment for 4 weeks (n=9). Closed circles represent the means, and error bars denote SEM. *P<0.01, significantly different from Ang II–infused *Apoe*$^{-/-}$ mice. E, Survival curves of *Apoe*$^{-/-}$ and *Apoe*$^{-/-}$*Hic-5*$^{-/-}$ mice during the Ang II treatment. *P<0.05 significantly different from *Apoe*$^{-/-}$ mice. F, Typical AAA rupture in Ang II–infused *Apoe*$^{-/-}$ mice. The arrows point to a hematoma in the abdominal cavity. G, Victoria Blue H&E (VBHE) stains of aortic cross sections from *Apoe*$^{-/-}$ and *Apoe*$^{-/-}$*Hic-5*$^{-/-}$ mice after Ang II infusion. The arrows indicate ruptured elastic lamina in *Apoe*$^{-/-}$ mice. Scale bars, 100 μm. AAA indicates abdominal aortic aneurysm; Ang II, angiotensin II; Hic-5, hydrogen peroxide–inducible clone 5.

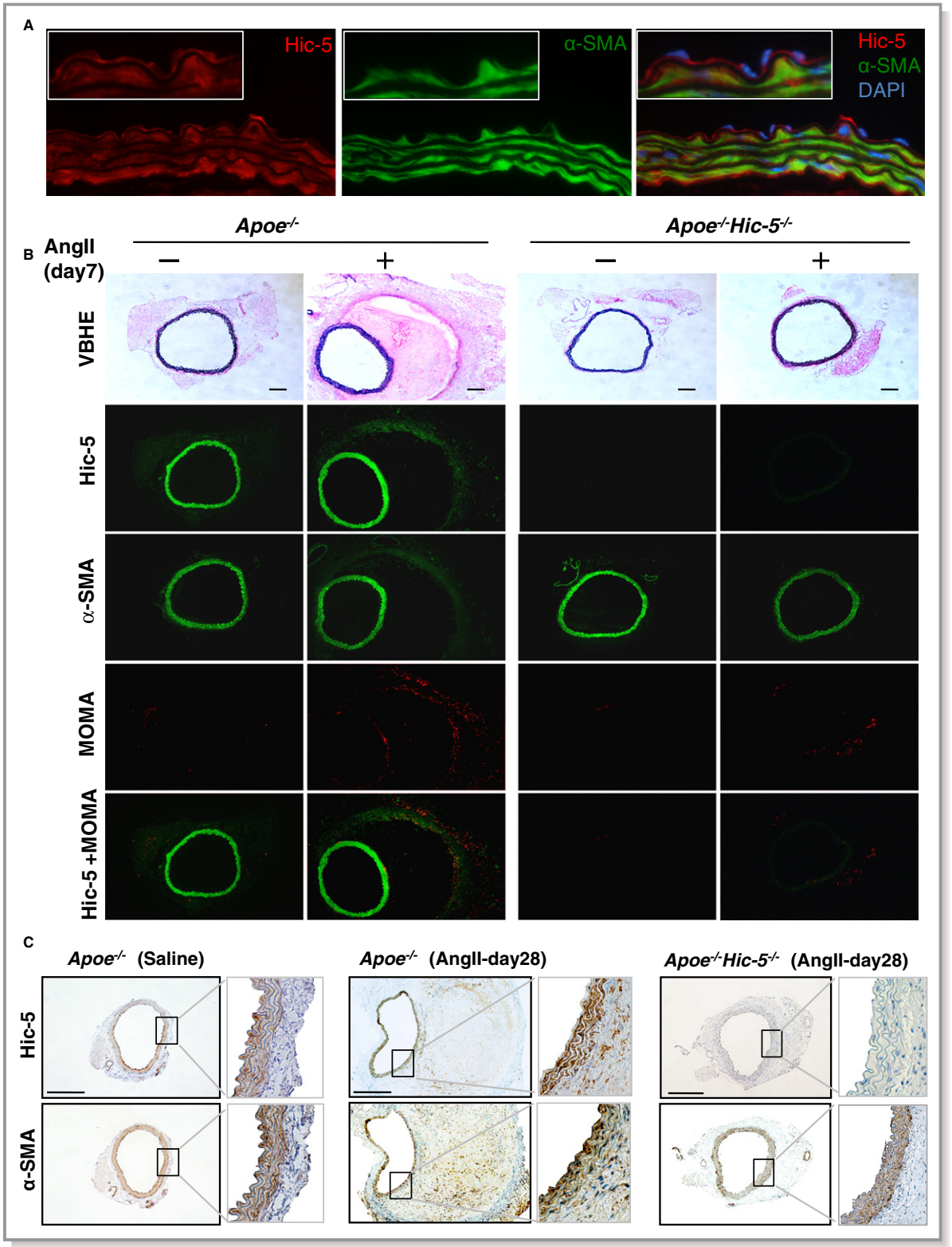

Figure 2. The expression of Hic-5 in the mouse aorta. A, Representative fluorescent immunostaining for Hic-5 (red), α–smooth muscle actin (α-SMA) (green), and DAPI for nucleus in aortic serial sections from *Apoe*$^{-/-}$. B, Representative VBHE staining elastin and fluorescent immunostaining for Hic-5 (green), α-SMA (green), and monocyte/macrophage (MOMA) (red) in aortic serial sections from *Apoe*$^{-/-}$ and *Apoe*$^{-/-}$*Hic-5*$^{-/-}$ mice after saline or Ang II infusion for 7 days. Scale bars, 200 μm. C, Representative immunostaining for Hic-5 and α-SMA in aortic cross sections from *Apoe*$^{-/-}$ and *Apoe*$^{-/-}$*Hic-5*$^{-/-}$ mice after saline or Ang II infusion for 4 weeks. AAA indicates abdominal aortic aneurysm; Ang II, angiotensin II; Hic-5, hydrogen peroxide–inducible clone 5; VBHE, Victoria Blue hematoxylin & eosin.

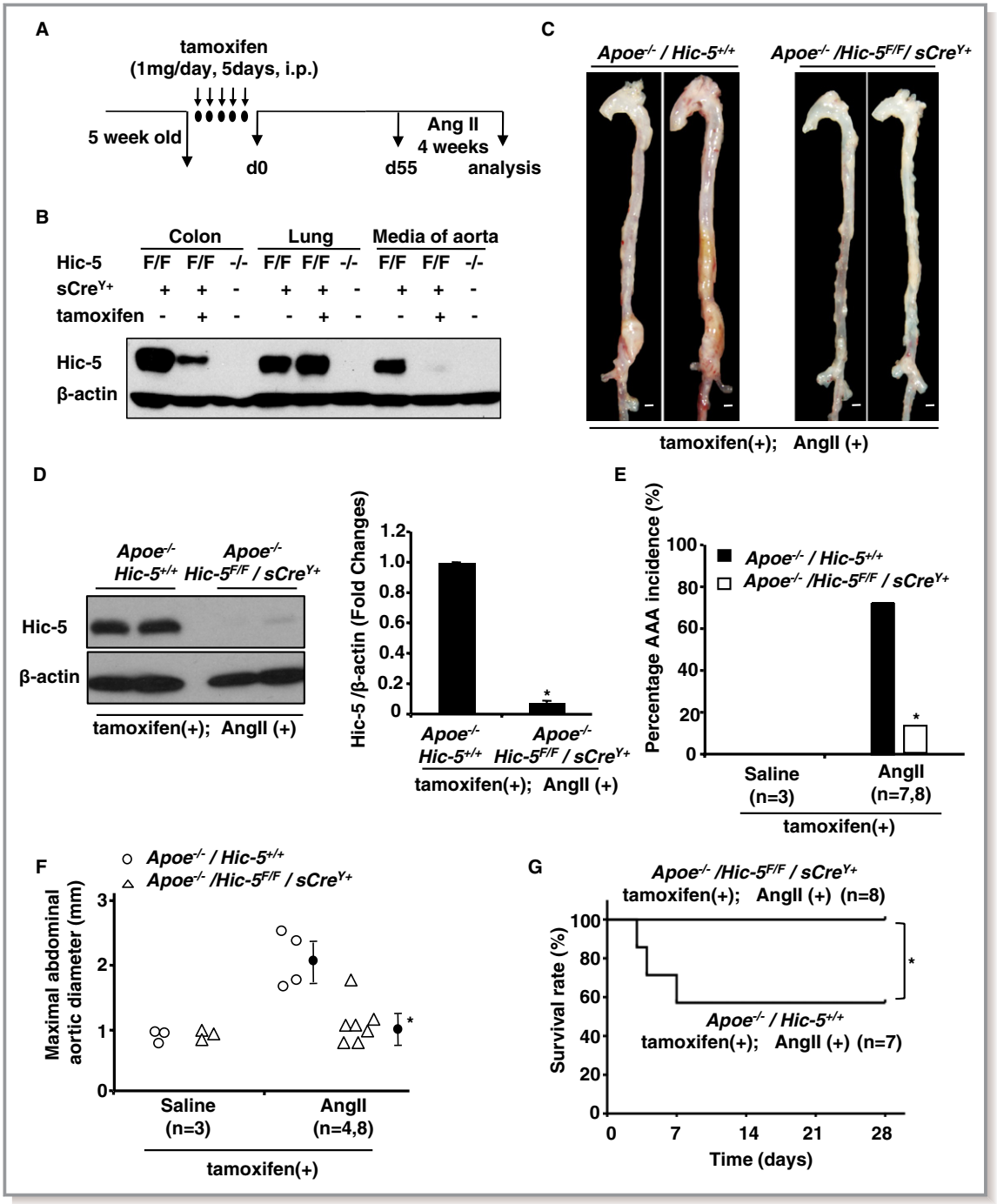

Figure 3. Smooth muscle–specific deletion of Hic-5 inhibited Ang II–infused AAA formation in vivo. A, Time scheme for the generation of smooth muscle–specific knockout mice for Hic-5 (*SM-Hic-5KO*). B, Immunoblots to assess the expression of Hic-5 in the colon, lung, and aortic media from *Hic-5*$^{-/-}$ and *Hic-5*$^{F/F}$/*sCre*$^{Y+}$ with or without the tamoxifen treatment. C, Representative aortas from *Apoe*$^{-/-}$*Hic-5*$^{+/+}$ and *Apoe*$^{-/-}$*Hic-5*$^{F/F}$/*sCre*$^{Y+}$ mice treated with Ang II after the tamoxifen injection. Scale bars, 1 mm. D, Immunoblots to analyze the expression of Hic-5 in the aortic media. Quantitative analyses of Hic-5 are shown in the right panel. *P<0.01 significantly different from *Apoe*$^{-/-}$*Hic-5*$^{+/+}$ mice. E, The incidence of Ang II–induced AAAs in *Apoe*$^{-/-}$*Hic-5*$^{+/+}$ (n=7) and *Apoe*$^{-/-}$*Hic-5*$^{F/F}$/*sCre*$^{Y+}$ (n=8) after the tamoxifen injection. *P<0.05 significantly different from *Apoe*$^{-/-}$*Hic-5*$^{+/+}$ mice. Saline infusion did not induce AAA formation in either group. F, Maximal diameters of abdominal aortas in both groups. Open circles represent *Apoe*$^{-/-}$*Hic-5*$^{+/+}$ mice; triangles represent *Apoe*$^{-/-}$*Hic-5*$^{F/F}$/*sCre*$^{Y+}$ mice. Closed circles represent the means, and error bars denote SEM. *P<0.01 significantly different from Ang II–infused *Apoe*$^{-/-}$ mice. G, Survival curve of both groups during the Ang II treatment after the tamoxifen injection. *P<0.05 significantly different from *Apoe*$^{-/-}$*Hic-5*$^{+/+}$ mice. AAA indicates abdominal aortic aneurysm; Ang II, angiotensin II; Hic-5, hydrogen peroxide–inducible clone 5.

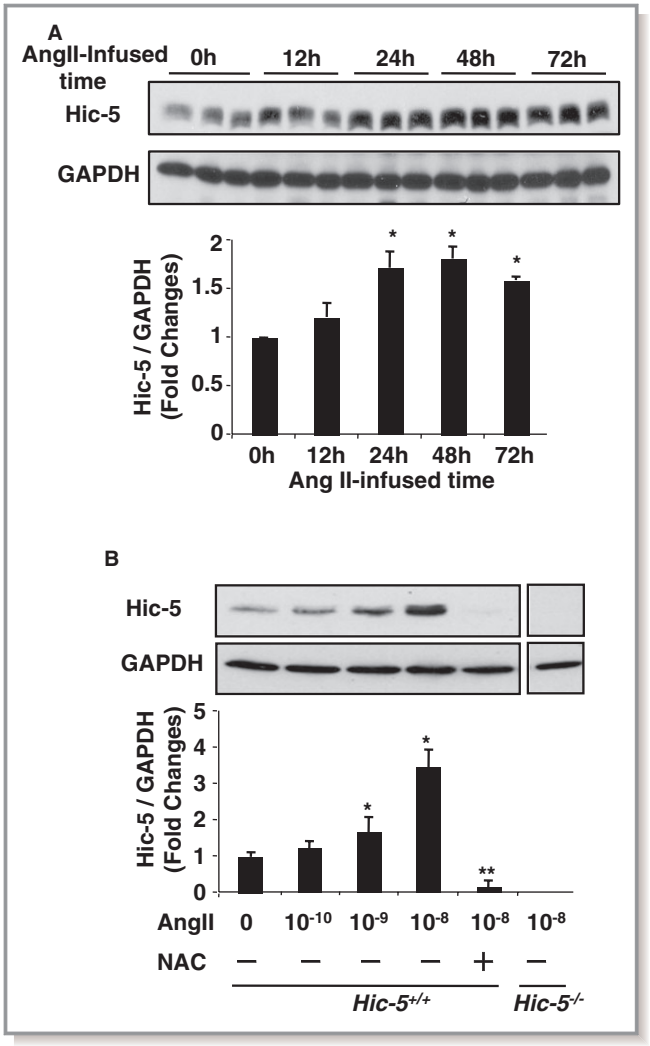

Figure 4. Ang II upregulated the expression of Hic-5 in the mouse aorta and cultured VSMCs. A, Immunoblot analysis of Hic-5 expression in the aortic media from Ang II–infused *Apoe*$^{-/-}$ mice at the indicated times. The lower panel shows quantitative analyses of Hic-5 expression after normalization with glyceraldehyde 3-phosphate dehydrogenase (GAPDH). B, Immunoblots to analyze the expression of Hic-5 in cultured *Hic-5*$^{+/+}$ VSMCs in response to Ang II with or without an ROS scavenger, 10 mmol/L *N*-acetyl L-cysteine (NAC). The lower panel shows the results of the densitometric analysis of immunoblots after normalization with GAPDH. Data are expressed as means±SEM of 3 independent experiments. **P*<0.01 significantly different from untreated controls; ***P*<0.01 significantly different from the Ang II 10^{-8} mol/L treatment without ROS scavengers. AAA indicates abdominal aortic aneurysm; Ang II, angiotensin II; Hic-5, hydrogen peroxide–inducible clone 5; ROS, reactive oxygen species; VSMCs, vascular smooth muscle cells.

for 7 days in *Apoe*$^{-/-}$ mice markedly increased the expression of proMMP2 and activated MMP2 in the aortic media (Figure 5A). The induction of these 2 MMP2 proteins by Ang II infusion was significantly weaker in *Apoe*$^{-/-}$*Hic-5*$^{-/-}$ mice than in *Apoe*$^{-/-}$ mice (Figure 5A and 5B). We next focused on MT1-MMP, a major activator of proMMP2. Basal expression of MT1-MMP was negligible in the aortic media from both *Apoe*$^{-/-}$ and *Apoe*$^{-/-}$ *Hic-5*$^{-/-}$ mice. The Ang II treatment increased MT1-MMP protein expression in both groups; however, the induction of MT1-MMP was significantly attenuated in *Apoe*$^{-/-}$*Hic-5*$^{-/-}$ mice (Figure 5A and 5C). Gelatin zymography of the aortas from *Apoe*$^{-/-}$ showed an increase in proMMP2 and activated MMP2. In contrast, Ang II–treated aortas from *Apoe*$^{-/-}$*Hic-5*$^{-/-}$ mice showed markedly reduced MMP2 expression and activation (Figure 5D). We obtained a similar result by in situ zymography, which showed that Ang II infusion markedly increased MMP activity in the medial layers of *Apoe*$^{-/-}$ mice but not in *Apoe*$^{-/-}$*Hic-5*$^{-/-}$ mice (Figure 5E). MMP activity was negligible in both *Apoe*$^{-/-}$ and *Apoe*$^{-/-}$*Hic-5*$^{-/-}$ mice after saline infusion (Figure 5E). We also observed that the Ang II treatment induced the expression of MT1-MMP and MMP2 in cultured VSMCs isolated from *Hic-5*$^{+/+}$ mice, whereas VSMCs from *Hic-5*$^{-/-}$ mice did not exhibit such an upregulation (Figure 5F and 5G). As shown with gelatin zymography, the secretion and activation of MMP2 in the culture media were lower in *Hic-5*$^{-/-}$ VSMCs than in *Hic-5*$^{+/+}$ VSMCs (Figure 5F, lower panel). In contrast to VSMCs, macrophages did not express Hic-5. As expected, no significant difference in MMP9 production was observed for macrophages from *Hic-5*$^{+/+}$ and *Hic-5*$^{-/-}$ mice (data not shown).

Hic-5 Regulated Phosphorylation of the JNK Pathway in VSMCs

We next analyzed the mechanism for decreases in MMP secretion and activation by Hic-5 deficiency. Although the enhanced production of ROS and associated vascular inflammation are known to accelerate Ang II–induced MMP induction and subsequent AAA development and progression,[2,5,26] we found that Hic-5 deficiency in *Apoe*$^{-/-}$ mice did not affect Ang II–induced ROS production or the secretion of proinflammatory cytokines and chemokines in cultured VSMCs and isolated aortas (data not shown).

The JNK pathway was previously shown to upregulate the expression of MMPs including MMP2 and MT1-MMP.[17,27] We next investigated whether Hic-5 was required for JNK activation by phosphorylation. VSMCs from *Hic-5*$^{+/+}$ and *Hic-5*$^{-/-}$ mice were treated with Ang II at the indicated times, and the phosphorylation of JNK was analyzed (Figure 6A). We used anisomycin, a potent stimulator of JNK, as a positive control.[28] Figure 5A showed no significant differences between *Hic-5*$^{+/+}$ and *Hic-5*$^{-/-}$ VSMCs in the phosphorylation of ERK1/2 and p38 after the Ang II treatment. However, Ang II–induced phosphorylation of JNK was markedly lower in *Hic-5*$^{-/-}$ VSMCs than in *Hic-5*$^{+/+}$ VSMCs, particularly in phosphorylation of p54 JNK, in which

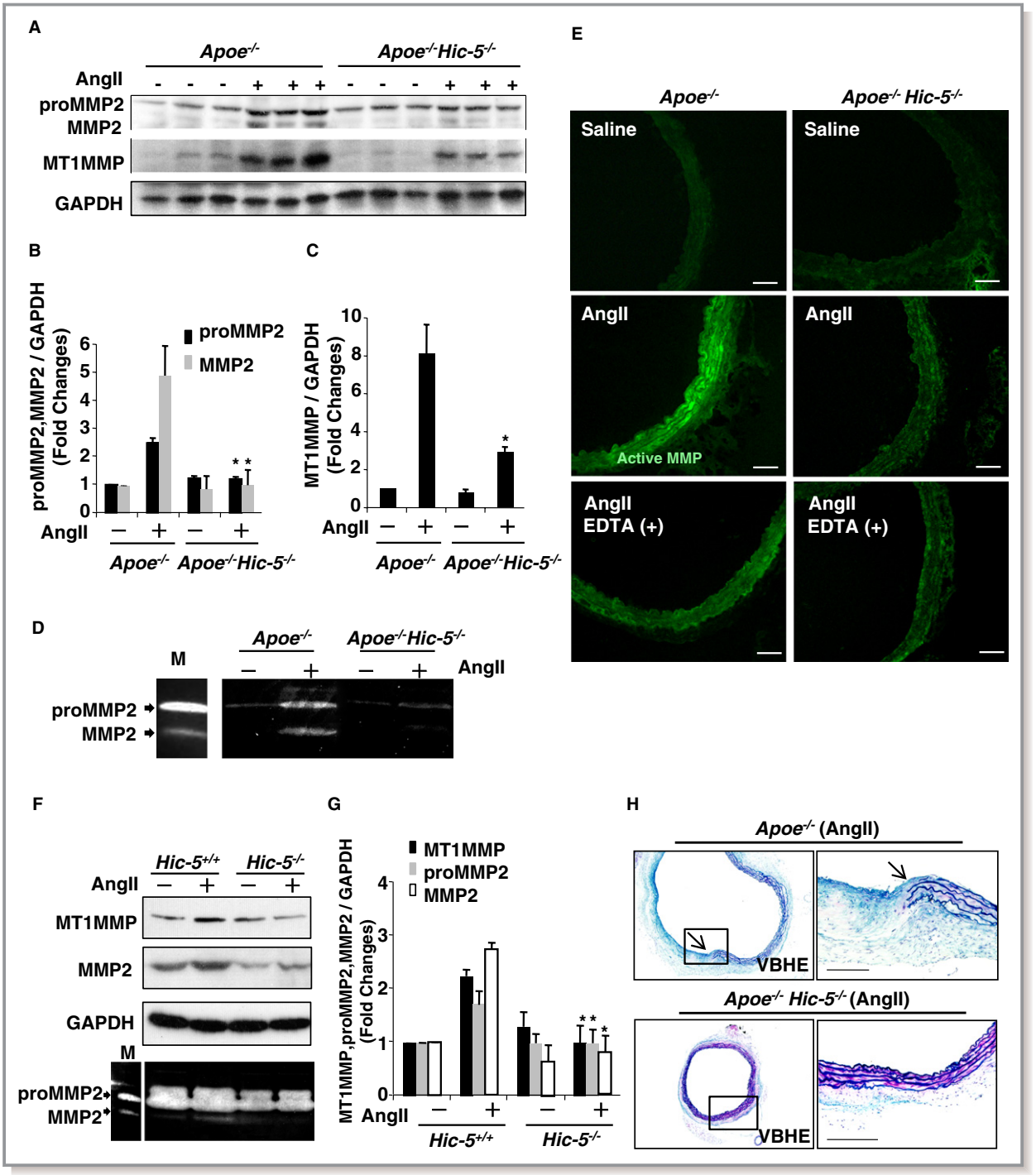

Figure 5. Ang II–induced MMP expression and activation were inhibited in the Hic-5$^{-/-}$ mouse aorta and cultured VSMCs. Representative immunoblots for proMMP2, MMP2, and MT1-MMP in the aortic media after Ang II infusion for 7 days (A) and immunoblots for MMP2 and MT1-MMP in cultured VSMCs after the Ang II treatment for 48 hours (F, upper 2 panels) in the indicated genotypes. (B, C, and G) Densitometric analyses of immunoblots for proMMP2, MMP2, and MT1-MMP after normalization with GAPDH. Data are expressed as means±SEM of 3 independent experiments. *P<0.01 significantly different from *Apoe*$^{-/-}$ mice (B and C) or *Hic-5*$^{+/+}$ VSMCs (G). Gelatin zymography of conditioned medium from the whole aorta organ culture (D) or cultured VSMCs (F, lowest panel) in the indicated genotypes. E, Aortas from *Apoe*$^{-/-}$ and *Apoe*$^{-/-}$*Hic-5*$^{-/-}$ mice infused with saline or Ang II for 7 days were analyzed by in situ zymography for gelatinase activity. Active MMPs are indicated by the green color. Scale bars, 50 μm. H, VBHE staining of aortas from *Apoe*$^{-/-}$ and *Apoe*$^{-/-}$*Hic-5*$^{-/-}$ mice 4 weeks after Ang II infusion. The arrows indicate degradation of the elastic lamina in *ApoE*$^{-/-}$ mice. AAA indicates abdominal aortic aneurysm; Ang II, angiotensin II; Hic-5, hydrogen peroxide–inducible clone 5; MMPs indicates matrix metalloproteinases; VBHE, Victoria Blue hematoxylin & eosin; VSMCs, vascular smooth muscle cells.

phosphorylation was almost completely suppressed even under anisomycin stimulation (Figure 6A and 6B). In vivo, the Ang II treatment of *Apoe*$^{-/-}$ mice for 7 days significantly induced the phosphorylation of JNK, as shown by Western blotting assay of the aortic media. In contrast, a marked reduction in the phosphorylation of JNK after Ang II infusion was observed in *Apoe*$^{-/-}$ *Hic-5*$^{-/-}$ mice (Figure 6C). We next restored Hic-5 expression in *Hic-5*$^{-/-}$ VSMCs through adenovirus-mediated gene transfer (Ad-hic-5/flag), using the β-galactosidase gene (Ad-β-gal) as a control. Compared with control gene, exogenous *Hic-5* (flag-tagged) expression in *Hic-5*$^{-/-}$ VSMCs efficiently restored basal and Ang II–induced phosphorylation of JNK, especially p54 JNK (Figure 6D). We next examined whether Hic-5 served as a component of the JNK pathway. JNK protein kinases are activated by phosphorylation by MKK4 and MKK7, which are well known as adjacent upstream kinases of JNK.[29,30] We found that Hic-5 deficiency hardly affected the phosphorylation of MKK7 (data not shown). However, the phosphorylation of MKK4 was significantly higher in *Hic-5*$^{-/-}$ VSMCs than in *Hic-5*$^{+/+}$ VSMCs, even at basal levels (Figure 6E).

Hic-5 Is Associated Directly With MKK4 and JNK

The specificity of signal transduction depends on specific protein–protein interactions. Scaffold proteins, including the JNK interacting protein group bind to MKK4 and/or MKK7, in addition to JNK, and coordinate signal transduction in the JNK pathway.[30,31] As described previously, Hic-5 serves as a scaffold of integrin signaling through interactions with multiple signaling molecules.[12] Because Hic-5 deficiency led to the decreased phosphorylation of p54 JNK and increased phosphorylation of MKK4, we reasoned that Hic-5 may serve as a scaffold protein between MKK4 and p54 JNK. To test this possibility, we performed immunoprecipitation experiments using an Hic-5–specific antibody and aortic tissue lysate from *Hic-5*$^{+/+}$ mice. The results showed that the Hic-5 antibody pulled down JNK, especially p54 JNK and MKK4, but not MKK7, p38, or ERK together with Hic-5 (Figure 7A). Using the specific antibody of JNK1 and JNK2, we found that JNK2 is primarily composed of the p54 JNK isoform in cultured mouse VSMCs (data not shown).

To further validate the association of Hic-5 with p54 JNK or MKK4 in *Hic-5*$^{+/+}$ VSMCs, we performed in situ proximity ligation assays, which identify the subcellular localization of interacting endogenous proteins within approximately 40 nm at single molecule resolution.[32] A fluorescent signal by this method (red dots) indicated the association of Hic-5 with p54 JNK or MMK4. Clear red spots were detected with the Hic-5 antibody in combination with the JNK2 antibody or MKK4 antibody in *Hic-5*$^{+/+}$ VSMCs, whereas only background staining was obtained with the Hic-5 antibody in combination with control IgG (Figure 7B). These results indicate that Hic-5 colocalized with p54 JNK and MKK4 within 40 nm in VSMCs. The colocalization of these molecules was further demonstrated by using an immunoelectron microscopic method in aortas from *Hic-5*$^{+/+}$ mice (Figure 7C). We next analyzed the interaction of Hic-5 with P-JNK or P-MKK4 in cultured *Hic-5*$^{+/+}$ VSMCs using PLA assays. More red fluorescent dots were detected with the Hic-5 antibody in combination with the P-JNK antibody or P-MKK4 antibody in VSMCs after Ang II treatment than in those detected with the control (untreated with Ang II) (Figure 7D), suggesting that Hic-5 also contributes to the association of P-JNK and P-MKK4 in VSMCs. Together, these results suggest that Hic-5 serves as a scaffold selective for p54 JNK and MKK4 in VSMCs and contributes to the activation of p54 JNK by binding to both MKK4 and p54 JNK (Figure 7E).

Discussion

We showed that Ang II–induced ROS promoted the expression of Hic-5 in VSMCs, which subsequently accelerated the phosphorylation of JNK, especially p54 JNK. Mechanistically, Hic-5 can bind to both p54 JNK and its upstream regulatory molecule, MKK4. Suppression of the p54 JNK pathway by Hic-5 loss resulted in the limited secretion of proMMP2 and MMP2 and expression of MT1-MMP, which led to protection from elastin degradation and subsequent AAA formation and rupture (Figure 8). This study not only identified Hic-5 as a downstream molecule of ROS, which promotes AAA formation, but also suggested that Hic-5 can serve as a specific scaffold between MKK4 and p54 JNK in VSMCs.

Although numerous studies have clearly demonstrated that ROS play an important role in the development of aneurysms, no strong therapeutic strategy currently exists for the clinical benefits of antioxidant administration. One potential reason for this could be the crucial role of ROS in mediating the transduction of intracellular signals that are also important for regulating both VSMC and vascular functions.[33,34] Our findings not only demonstrated that Hic-5, as a downstream molecule of ROS in the transduction of intracellular signals, regulates AAA development but also that its absence did not affect ROS production or normal function in mice. In addition, Hic-5 specifically binds to p54 JNK and its upstream molecule, MKK4, and plays an essential role in the phosphorylation of p54 JNK in VSMCs. Although the inhibition of JNKs has been considered as a potential therapeutic target for aneurysms,[17] JNKs have been shown to play critical roles in adult tissue homeostasis. In fact, the knockout of both *Jnk1* and *Jnk2* genes in mice was shown to be an embryonic lethal mutation.[35] Thus, targeting JNKs themselves may be limited to be used as a mainstream treatment approach. Therefore, the exact JNK isoform (JNK1

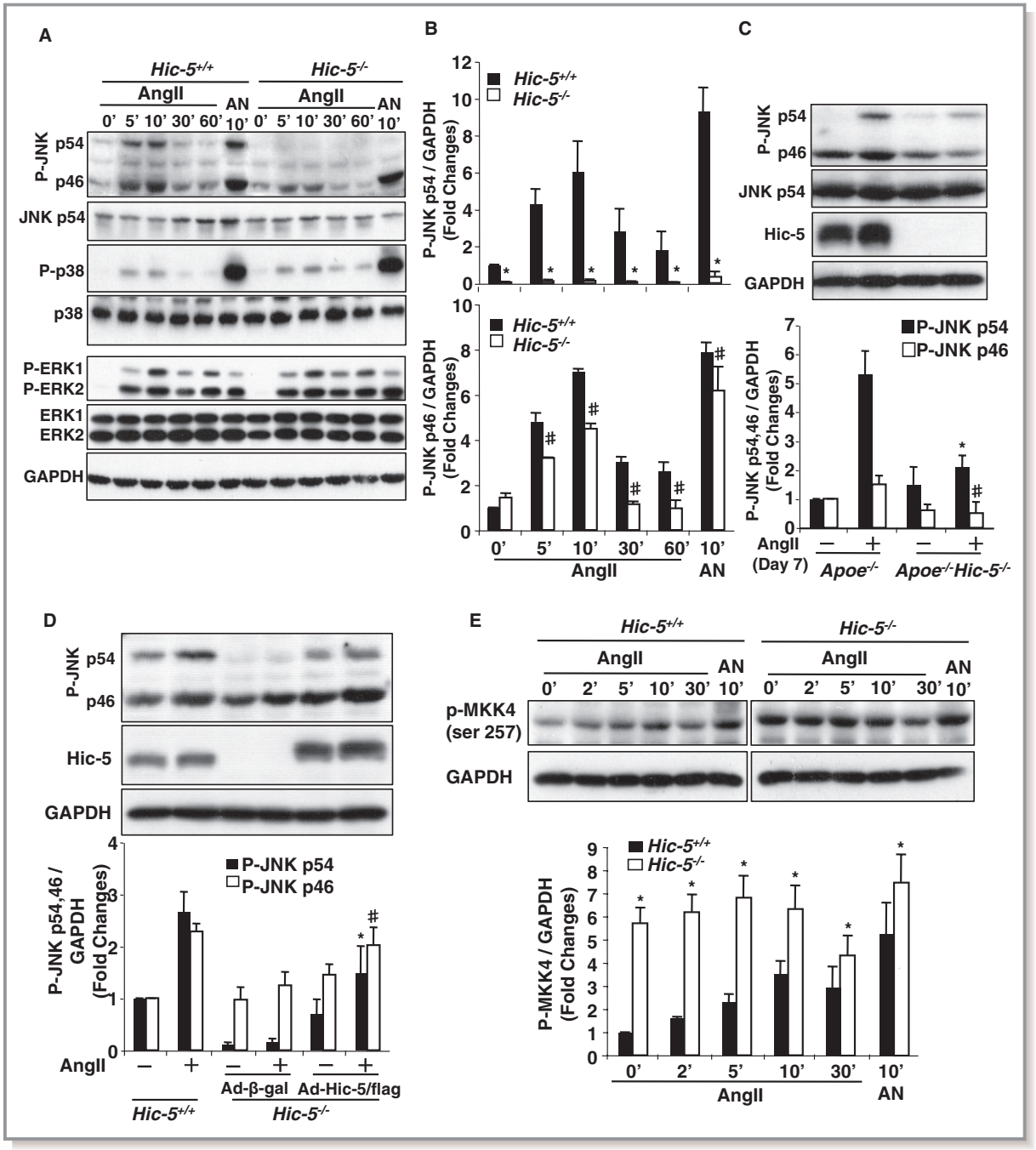

Figure 6. Hic-5 deficiency inhibited the phosphorylation of c-Jun N-terminal kinase (JNK) in VSMCs. A, Representative immunoblots of VSMCs are shown for MAP kinases (ERK, p38, and JNK) and for their phosphorylated forms (P-ERK, P-p38, and P-p54/p46 JNK, respectively) in the indicated genotypes after the Ang II (10^{-7} mol/L) or anisomycin (AN; 20 μg/mL) treatment. B, Quantitative analyses of P-p54/p46 JNK are shown after normalization with GAPDH. C, Phosphorylation of p54/p46 JNK was detected using mouse aortas from Ang II–infused *Apoe*$^{-/-}$ and *Apoe*$^{-/-}$*Hic-5*$^{-/-}$ mice for 7 days. Quantitative analyses of P-p54/p46 JNK are shown in the lower panel. D, Adenovirus-mediated expression of flag-tagged *Hic-5* (Ad-Hic-5/flag) in *Hic-5*$^{-/-}$ VSMCs induced the phosphorylation of p54/p46 JNK. *Hic-5*$^{-/-}$ VSMCs were infected with Ad-Hic-5/flag or the adenovirus-mediated β-galactosidase gene (Ad-β-gal) as a control. After 12 hours of infection, the expression of P-JNK and Hic-5 with or without the Ang II treatment was analyzed by immunoblots. E, Enhanced phosphorylation of MKK4 in *Hic-5*$^{-/-}$ VSMCs. The levels of MKK4 phosphorylation induced by Ang II were detected at each of the indicated times. AN was used as a positive control. All results are means±SEM of 3 independent experiments. **P*<0.01, $^{\#}$*P*<0.05 significantly different from *Hic-5*$^{+/+}$ VSMCs (B and E) or *Apoe*$^{-/-}$*Hic-5*$^{+/+}$ mice (C) or infected with Ad-β-gal gene (D). AAA indicates abdominal aortic aneurysm; Ang II, angiotensin II; Hic-5, hydrogen peroxide–inducible clone 5; JNK, Jun N-terminal kinase; MKK, mitogen-activated protein kinase; VSMCs, vascular smooth muscle cells.

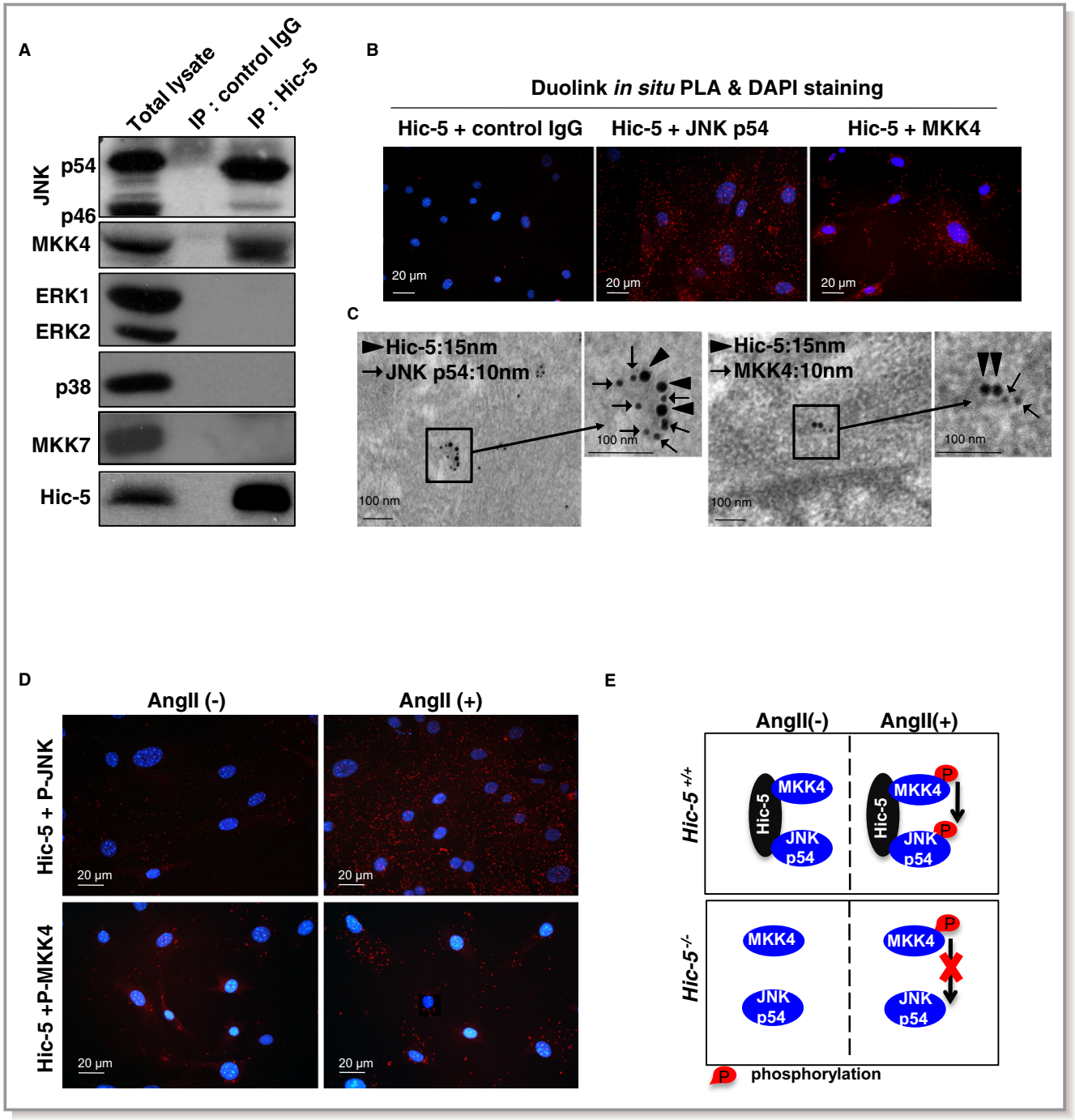

Figure 7. Hic-5 interacted with p54 JNK and MKK4 in VSMCs. Coimmunoprecipitation of p54 JNK and MKK4 with the Hic-5 antibody in the mouse aorta. Immunoblots for p54/p46 JNK, MKK4, ERK1/2, p38, MKK7, and Hic-5 in the total lysates of the mouse aorta or that after immunoprecipitation with the Hic-5–specific antibody or nonimmune mouse IgG as a negative control. IP, immunoprecipitation. B, Interaction of endogenous Hic-5 and p54 JNK or MKK4 in cultured *Hic-5*$^{+/+}$ VSMCs. PLA was carried out to detect the proximal location of Hic-5 and p54 JNK or that of Hic-5 and MKK4 (shown as red dots) as described in "Methods." All samples were stained with DAPI (blue) to visualize nuclei. C, Immunogold electron microscopy of *Hic-5*$^{+/+}$ mouse aortas was performed. Co-localization of Hic-5 with p54 JNK or that with MKK4 in mouse aortic SMCs was detected using secondary antibodies conjugated with larger (15-nm) gold colloids for Hic-5 (arrowheads) and smaller (10-nm) gold colloids for p54 JNK or MKK4 (arrows), respectively. D, Interaction of Hic-5 with P-JNK or that with P-MKK4 in cultured *Hic-5*$^{+/+}$ VSMCs with or without the Ang II treatment as demonstrated by the PLA method. E, Schematic diagram summarizing the interaction of Hic-5 and p54 JNK or MKK4 in VSMCs. Red circles represent phosphorylation. Arrows indicate signal transduction for p54 JNK phosphorylation after the Ang II treatment. The red X-mark represents inhibited signal transduction by Hic-5 deficiency. AAA indicates abdominal aortic aneurysm; Ang II, angiotensin II; Hic-5, hydrogen peroxide–inducible clone 5; JNK, Jun *N*-terminal kinase; MKK, mitogen-activated protein kinase; PLA, proximity ligation assay.

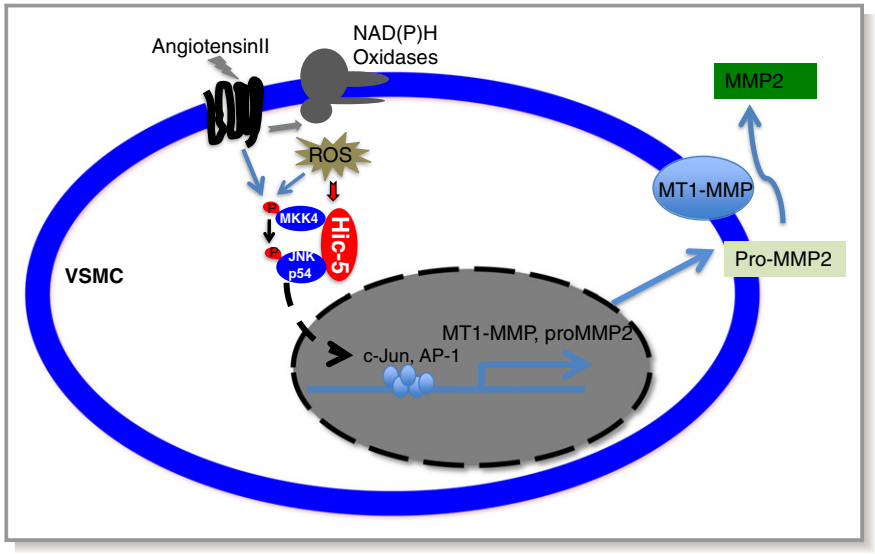

Figure 8. Ang II–induced AAA formation via Hic-5 in mice. Ang II binds to its receptors and induces the production of ROS in VSMCs. Ang II–induced ROS promote the expression of Hic-5 in VSMCs and Hic-5 serves as a specific scaffold between JNK p54 and its upstream molecule, MKK4, which contributes to the transmission of the activated signal from MKK4 to JNKp54. The loss of Hic-5 suppresses the JNK p54 pathway and results in the limited expression of proMMP2 and MT1-MMP and activation of MMP2. AAA indicates abdominal aortic aneurysm; Ang II, angiotensin II; Hic-5, hydrogen peroxide–inducible clone 5; JNK, Jun N-terminal kinase; MMP, matrix metalloproteinase; MKK, mitogen-activated protein kinase; ROS, reactive oxygen species.

or JNK2) is required to be identified in aneurysm formation. We found that JNK2 is primarily composed of the p54 JNK isoform in cultured mouse VSMCs. In addition, *Jnk2* deficiency in mouse VSMCs markedly inhibited the secretion of MMP2.[17] All these suggest that Hic-5–targeted therapy may be more specific for the treatment of aneurysms with minimum side effects.

Paxillin, a member of paxillin family proteins together with Hic-5, has extensive homology with Hic-5 and is known to provide an efficient scaffold for the ERK module.[36] In the present study, we demonstrated that Hic-5 served as a scaffold for the p54 JNK module. These results raise the possibility that each paxillin family protein may behave as a respective scaffold for one of the MAPK modules.

We also found that Hic-5 expressed in VSMCs, rather than other types of cells, was essential for the development of AAAs. A couple of molecules expressed in VSMCs have been proposed to initiate AAA development by promoting the secretion of MMP2 and inflammatory cell recruitment in aneurysm formation in mice and humans.[9,25,37] These studies strongly support our findings that VSMC-derived Hic-5 played a key role in the initiation of AAAs by promoting the secretion and activation of MMP2. Moreover, our results showed that Hic-5 was induced in the aorta in the early stage of Ang II–induced AAA formation. Although the Ang II–induced vascular inflammatory response contributes to AAA progression, Hic-5 deficiency did not affect the secretion of proinflammatory cytokines in VSMCs, and Hic-5 was also not expressed in mouse macrophages. In light of these findings, Hic-5 may not play a major role in inflammatory responses in AAA development.

It has been previously reported that there are differences between human AAAs and Ang II–induced mouse AAAs including their location in the infrarenal versus suprarenal region, respectively; and aortic dissection is an early event in Ang II–induced mouse AAAs but not in human AAAs.[19] Previous studies have shown that an Ang II receptor blocker prevented aortic aneurysm dilatation in mouse and human Marfan syndrome (MFS).[38,39] One of the major clinical manifestations of MFS is aortic aneurysm. Fibrillin-1 has been identified as the gene responsible for MFS.[40] Recently, elevated circulating TGF-β1 concentrations and the critical role of TGF-β–activated MAPK signaling were reported in human and mouse MFS, respectively.[41,42] Hic-5 was originally identified as a TGF-β1–inducible gene; moreover, the Gene Coexpression Database, which is a database of comparative gene coexpression networks in mammals (http://www.coxpresdb.jp/),[43] revealed that fibrillin-1 and Hic-5 were spatiotemporally coexpressed in mice and humans. Therefore, it is reasonable to speculate that Hic-5 may play a key role in the development of MFS together with fibrillin-1. Future studies should focus on the role of Hic-5 in MFS using an appropriate animal model.

The current study demonstrated that Hic-5 deficiency resulted in the effective suppression of AAAs in an animal model. Hic-5–targeted therapy may provide a novel therapeutic option for the treatment of AAAs in the future.

Sources of Funding

This work was supported by Grants-in-Aid for Young Scientists (B) (24791396 to X.-F. Lei and 23791090 to J.-r. Kim-Kaneyama), Scientific Research (C) (23591341 to T. Miyazaki) from The Ministry of Education, Culture, Sports, Science and Technology of Japan, Showa University Medical Foundation, Japan-China Medical Association, and Japan Heart Foundation Dr Hiroshi Irisawa & Aya Irisawa Memorial Research Grant (to J.-r. Kim-Kaneyama). This work was also supported in part by the MEXT (Ministry of Education, Culture, Sports, Science and Technology)-Supported Program for the Strategic Research Foundation at Private Universities, 2012–2016.

Disclosures

None.

References

1. Stanley JC, Barnes RW, Ernst CB, Hertzer NR, Mannick JA, Moore WS. Vascular surgery in the united states: workforce issues. Report of the society for vascular surgery and the international society for cardiovascular surgery, north american chapter, committee on workforce issues. *J Vasc Surg*. 1996;23:172–181.
2. McCormick ML, Gavrila D, Weintraub NL. Role of oxidative stress in the pathogenesis of abdominal aortic aneurysms. *Arterioscler Thromb Vasc Biol*. 2007;27:461–469.
3. Miller FJ Jr, Sharp WJ, Fang X, Oberley LW, Oberley TD, Weintraub NL. Oxidative stress in human abdominal aortic aneurysms: a potential mediator of aneurysmal remodeling. *Arterioscler Thromb Vasc Biol*. 2002;22:560–565.
4. Gavazzi G, Deffert C, Trocme C, Schappi M, Herrmann FR, Krause KH. NOX1 deficiency protects from aortic dissection in response to angiotensin II. *Hypertension*. 2007;50:189–196.
5. Thomas M, Gavrila D, McCormick ML, Miller FJ Jr, Daugherty A, Cassis LA, Dellsperger KC, Weintraub NL. Deletion of p47phox attenuates angiotensin ii-induced abdominal aortic aneurysm formation in apolipoprotein E-deficient mice. *Circulation*. 2006;114:404–413.
6. Xiong W, Mactaggart J, Knispel R, Worth J, Zhu Z, Li Y, Sun Y, Baxter BT, Johanning J. Inhibition of reactive oxygen species attenuates aneurysm formation in a murine model. *Atherosclerosis*. 2009;202:128–134.
7. Longo GM, Xiong W, Greiner TC, Zhao Y, Fiotti N, Baxter BT. Matrix metalloproteinases 2 and 9 work in concert to produce aortic aneurysms. *J Clin Invest*. 2002;110:625–632.
8. Hellenthal FA, Buurman WA, Wodzig WK, Schurink GW. Biomarkers of AAA progression. Part 1: extracellular matrix degeneration. *Nat Rev Cardiol*. 2009;6:464–474.
9. Satoh K, Nigro P, Matoba T, O'Dell MR, Cui Z, Shi X, Mohan A, Yan C, Abe J, Illig KA, Berk BC. Cyclophilin A enhances vascular oxidative stress and the development of angiotensin II-induced aortic aneurysms. *Nat Med*. 2009;15:649–656.
10. Shibanuma M, Mashimo J, Kuroki T, Nose K. Characterization of the TGF beta 1-inducible hic-5 gene that encodes a putative novel zinc finger protein and its possible involvement in cellular senescence. *J Biol Chem*. 1994;269:26767–26774.
11. Kim-Kaneyama JR, Takeda N, Sasai A, Miyazaki A, Sata M, Hirabayashi T, Shibanuma M, Yamada G, Nose K. Hic-5 deficiency enhances mechanosensitive apoptosis and modulates vascular remodeling. *J Mol Cell Cardiol*. 2011;50:77–86.
12. Kim-Kaneyama JR, Lei XF, Arita S, Miyauchi A, Miyazaki T, Miyazaki A. Hydrogen peroxide-inducible clone 5 (hic-5) as a potential therapeutic target for vascular and other disorders. *J Atheroscler Thromb*. 2012;19:601–607.
13. Wirth A, Benyo Z, Lukasova M, Leutgeb B, Wettschureck N, Gorbey S, Orsy P, Horvath B, Maser-Gluth C, Greiner E, Lemmer B, Schutz G, Gutkind JS, Offermann S. G12-g13-larg-mediated signaling in vascular smooth muscle is required for salt-induced hypertension. *Nat Med*. 2008;14:64–68.
14. Daugherty A, Manning MW, Cassis LA. Angiotensin II promotes atherosclerotic lesions and aneurysms in apolipoprotein E-deficient mice. *J Clin Invest*. 2000;105:1605–1612.
15. Sun J, Sukhova GK, Yang M, Wolters PJ, MacFarlane LA, Libby P, Sun C, Zhang Y, Liu J, Ennis TL, Knispel R, Xiong W, Thompson RW, Baxter BT, Shi GP. Mast cells modulate the pathogenesis of elastase-induced abdominal aortic aneurysms in mice. *J Clin Invest*. 2007;117:3359–3368.
16. Soderberg O, Gullberg M, Jarvius M, Ridderstrale K, Leuchowius KJ, Jarvius J, Wester K, Hydbring P, Bahram F, Larsson LG, Landegren U. Direct observation of individual endogenous protein complexes in situ by proximity ligation. *Nat Methods*. 2006;3:995–1000.
17. Yoshimura K, Aoki H, Ikeda Y, Fujii K, Akiyama N, Furutani A, Hoshii Y, Tanaka N, Ricci R, Ishihara T, Esato K, Hamano K, Matsuzaki M. Regression of abdominal aortic aneurysm by inhibition of c-Jun N-terminal kinase. *Nat Med*. 2005;11:1330–1338.
18. Kim-Kaneyama JR, Wachi N, Sata M, Enomoto S, Fukabori K, Koh K, Shibanuma M, Nose K. Hic-5, an adaptor protein expressed in vascular smooth muscle cells, modulates the arterial response to injury in vivo. *Biochem Biophys Res Commun*. 2008;376:682–687.
19. Saraff K, Babamusta F, Cassis LA, Daugherty A. Aortic dissection precedes formation of aneurysms and atherosclerosis in angiotensin II-infused, apolipoprotein E-deficient mice. *Arterioscler Thromb Vasc Biol*. 2003;23:1621–1626.
20. Bourassa PA, Milos PM, Gaynor BJ, Breslow JL, Aiello RJ. Estrogen reduces atherosclerotic lesion development in apolipoprotein E-deficient mice. *Proc Natl Acad Sci USA*. 1996;93:10022–10027.
21. Griendling KK, Minieri CA, Ollerenshaw JD, Alexander RW. Angiotensin II stimulates nadh and nadph oxidase activity in cultured vascular smooth muscle cells. *Circ Res*. 1994;74:1141–1148.
22. Zafari AM, Ushio-Fukai M, Akers M, Yin Q, Shah A, Harrison DG, Taylor WR, Griendling KK. Role of NADH/NADPH oxidase-derived H_2O_2 in angiotensin II-induced vascular hypertrophy. *Hypertension*. 1998;32:488–495.
23. Visse R, Nagase H. Matrix metalloproteinases and tissue inhibitors of metalloproteinases: structure, function, and biochemistry. *Circ Res*. 2003;92:827–839.
24. Luchtefeld M, Grote K, Grothusen C, Bley S, Bandlow N, Selle T, Struber M, Haverich A, Bavendiek U, Drexler H, Schieffer B. Angiotensin II induces MMP-2 in a p47phox-dependent manner. *Biochem Biophys Res Commun*. 2005;328:183–188.
25. Wang S, Zhang C, Zhang M, Liang B, Zhu H, Lee J, Viollet B, Xia L, Zhang Y, Zou MH. Activation of AMP-activated protein kinase alpha2 by nicotine instigates formation of abdominal aortic aneurysms in mice in vivo. *Nat Med*. 2012;18:902–910.
26. Tieu BC, Lee C, Sun H, Lejeune W, Recinos A III, Ju X, Spratt H, Guo DC, Milewicz D, Tilton RG, Brasier AR. An adventitial IL-6/MCP1 amplification loop accelerates macrophage-mediated vascular inflammation leading to aortic dissection in mice. *J Clin Invest*. 2009;119:3637–3651.
27. Ispanovic E, Haas TL. JNK and PI3k differentially regulate MMP-2 and MT1-MMP mRNA and protein in response to actin cytoskeleton reorganization in endothelial cells. *Am J Physiol Cell Physiol*. 2006;291:C579–C588.
28. Schmitz U, Ishida T, Ishida M, Surapisitchat J, Hasham MI, Pelech S, Berk BC. Angiotensin II stimulates p21-activated kinase in vascular smooth muscle cells: role in activation of JNK. *Circ Res*. 1998;82:1272–1278.
29. Haeusgen W, Herdegen T, Waetzig V. The bottleneck of JNK signaling: molecular and functional characteristics of MKK4 and MKK7. *Eur J Cell Biol*. 2011;90:536–544.
30. Davis RJ. Signal transduction by the JNK group of map kinases. *Cell*. 2000;103:239–252.
31. Dhanasekaran DN, Kashef K, Lee CM, Xu H, Reddy EP. Scaffold proteins of map-kinase modules. *Oncogene*. 2007;26:3185–3202.
32. Fredriksson S, Gullberg M, Jarvius J, Olsson C, Pietras K, Gustafsdottir SM, Ostman A, Landegren U. Protein detection using proximity-dependent DNA ligation assays. *Nat Biotechnol*. 2002;20:473–477.
33. Martin-Garrido A, Gonzalez-Ramos M, Griera M, Guijarro B, Cannata-Andia J, Rodriguez-Puyol D, Rodriguez-Puyol M, Saura M. H_2O_2 regulation of vascular function through sGC mRNA stabilization by HuR. *Arterioscler Thromb Vasc Biol*. 2011;31:567–573.

34. Sundaresan M, Yu ZX, Ferrans VJ, Irani K, Finkel T. Requirement for generation of H_2O_2 for platelet-derived growth factor signal transduction. *Science*. 1995;270:296–299.
35. Kuan CY, Yang DD, Samanta Roy DR, Davis RJ, Rakic P, Flavell RA. The JNK1 and JNK2 protein kinases are required for regional specific apoptosis during early brain development. *Neuron*. 1999;22:667–676
36. Ishibe S, Joly D, Zhu X, Cantley LG. Phosphorylation-dependent paxillin-ERK association mediates hepatocyte growth factor-stimulated epithelial morphogenesis. *Mol Cell*. 2003;12:1275–1285.
37. Hofmann Bowman M, Wilk J, Heydemann A, Kim G, Rehman J, Lodato JA, Raman J, McNally EM. S100A12 mediates aortic wall remodeling and aortic aneurysm. *Circ Res*. 2010;106:145–154
38. Groenink M, den Hartog AW, Franken R, Radonic T, de Waard V, Timmermans J, Scholte AJ, van den Berg MP, Spijkerboer AM, Marquering HA, Zwinderman AH, Mulder BJ. Losartan reduces aortic dilatation rate in adults with marfan syndrome: a randomized controlled trial. *Eur Heart J*. 2013;34:3491–3500.
39. Habashi JP, Judge DP, Holm TM, Cohn RD, Loeys BL, Cooper TK, Myers L, Klein EC, Liu G, Calvi C, Podowski M, Neptune ER, Halushka MK, Bedja D, Gabrielson K, Rifkin DB, Carta L, Ramirez F, Huso DL, Dietz HC. Losartan, an AT1 antagonist, prevents aortic aneurysm in a mouse model of marfan syndrome. *Science*. 2006;312:117–121.
40. Pearson GD, Devereux R, Loeys B, Maslen C, Milewicz D, Pyeritz R, Ramirez F, Rifkin D, Sakai L, Svensson L, Wessels A, Van Eyk J, Dietz HC. Report of the national heart, lung, and blood institute and national marfan foundation working group on research in marfan syndrome and related disorders. *Circulation*. 2008;118:785–791.
41. Matt P, Schoenhoff F, Habashi J, Holm T, Van Erp C, Loch D, Carlson OD, Griswold BF, Fu Q, De Backer J, Loeys B, Huso DL, McDonnell NB, Van Eyk JE, Dietz HC. Circulating transforming growth factor-beta in marfan syndrome. *Circulation*. 2009;120:526–532.
42. Holm TM, Habashi JP, Doyle JJ, Bedja D, Chen Y, van Erp C, Lindsay ME, Kim D, Schoenhoff F, Cohn RD, Loeys BL, Thomas CJ, Patnaik S, Marugan JJ, Judge DP, Dietz HC. Noncanonical TGFbeta signaling contributes to aortic aneurysm progression in marfan syndrome mice. *Science*. 2011;332:358–361.
43. Obayashi T, Hayashi S, Shibaoka M, Saeki M, Ohta H, Kinoshita K. Coxpresdb: a database of coexpressed gene networks in mammals. *Nucleic Acids Res*. 2008;36:D77–D82.